APPENDIX 3.5.B

JINR participation in the CLICdp collaboration

1 Introduction

The main activity of the JINR group in the CLICdp collaboration will be the preparation of the program of physics research at the CLIC collider. In addition to this, JINR group will be involved in service work usual for any collaboration: validation of physics software, participation in publication and speaker's Committees, preparation of common papers, representation of the Collaboration at conferences and workshops.

For the preparation of the CLIC research program, JINR group plans to carry out the following studies:

1. Precision measurement of the QED process $e^+e^- \to \gamma\gamma$ and setting limits on the new physics models

2. Precision measurement of the Higgs boson mass

3. Measurement of the top quark polarization and determination of the anomalous top form-factors

4. Measurement of $\gamma\gamma \to W^+W^-$ and $\gamma\gamma \to ZZ$ scattering and search for anomalous quartic coupling

The above studies will be based on the full CLICdp detector simulation and reconstruction software. Both signal and background Monte-Carlo

simulation will be used. The goal of the study is to demonstrate the possibility of the given measurement and to estimate the experimental precision that can be achieved with the full CLIC data sample. The proposed studies are detailed below.

2 Precision measurement of $e^+e^- \to \gamma\gamma$ annihilation

The reaction $e^+e^- \to \gamma\gamma$ (Fig.1) is the simplest QED process which can be predicted theoretically with very high precision. Experimentally it can be measured with very high precision as well, because the annihilation cross-section is rather large and the final state is extremely simple and unambiguous.
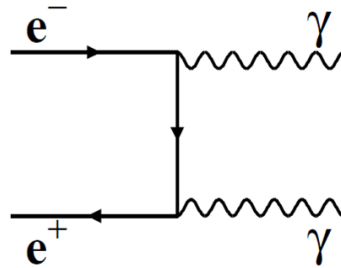

Figure 1: The lowest-order diagram for the $e^+e^- \to \gamma\gamma$ annihilation.

The final state is characterized by two very energetic showers in the electromagnetic calorimeter. A presence of a third, typically low-energy shower from an ISR photon is possible. No tracks of energetic charged particles are expected in the tracking detectors, except the rare cases of γ conversion which can be identified with rather good efficiency.

To search for new physics one has to compare the experimental results with the Standard Model predictions both for total and for differential cross-sections. In QED the differential cross-section of the $e^+e^- \to \gamma\gamma$ annihilation at Born level is expressed [1] as:

$$\left(\frac{d\sigma}{d\Omega}\right)_{\mathrm{Born}} = \frac{\alpha^2}{s}\left[\frac{1+\beta^2+\beta^2\sin^2\theta}{1-\beta^2\cos^2\theta} - \frac{2\beta^4\sin^4\theta}{(1-\beta^2\cos^2\theta)^2}\right] \approx \frac{\alpha^2}{s}\frac{1+\cos^2\theta}{1-\cos^2\theta},$$
(1)

where β is the speed of the beam electron and θ is the angle between the outcoming photon and the beamline. The angular distribution of the $e^+e^- \to \gamma\gamma$ events is illustrated in Fig.2. The blue curve shows the Standard Model prediction, points with errors correspond to the number of events expected with 1000 fb^{-1} integrated luminosity for CLIC running at 3 TeV, and the red curves correspond to $\pm$ 4 TeV QED cut-off parameter (see below).
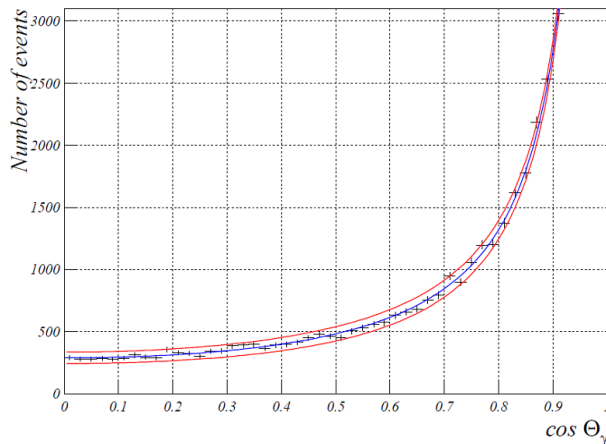

Figure 2: Angular distribution of the photons in $e^+e^- \to \gamma\gamma$ events.

The differential cross-section is very strongly peaked toward small scattering angles, it even becomes divergent if the beam particles are assumed to have the speed of light. As a consequence, the visible total cross-section strongly depends on the angular acceptance of the experimental set-up. To collect good statics it is vital to have tracking and calorimetric information close to the beam line. The CLICdp detector is perfectly suited for this goal, covering the forward region down to the polar angles $\theta \sim 10°$.

The process $e^+e^- \rightarrow \gamma\gamma$ is sensitive to various models of new physics beyond the Standard Model (BSM). Currently we plan to study the CLIC sensitivity to four such BSM models, which are briefly mentioned below.

The QED cut-off is the simplest BSM extension of QED. It postulates a finite size of the electron, which is equivalent to a short-range deviation from the Coulomb field parametrized by energy cut-off parameters $\Lambda_\pm$ [2]. The differential cross-section of the $e^+e^- \rightarrow \gamma\gamma$ process is modified in the following way:

$$\frac{d\sigma}{d\Omega} = \left(\frac{d\sigma}{d\Omega}\right)_{\text{Born}} \pm \frac{\alpha^2 s}{2\Lambda_\pm^4}(1 + \cos^2\theta) \qquad (2)$$

The effective Lagrangian theory [3] is another way to introduce the anomalous effects. The dimension-6 Lagrangian results in an anomalous term equivalent to the QED cut-off, while dimension-7 and dimension-8 Lagrangians introduce $ee\gamma\gamma$ contact interaction which adds an angular-independent term to the Born cross-section:

$$\frac{d\sigma}{d\Omega} = \left(\frac{d\sigma}{d\Omega}\right)_{\text{Born}} + \frac{s^2}{16}\frac{1}{\Lambda'^6}, \qquad (3)$$

where Λ' is the effective scale of the new physics.

Compactified extra dimensions is the concept [4] which assumes that the space-time has more than just 4 dimensions. The extra dimensions are compactified and hold Kaluza-Klein excitations which may produce observable effects. The model can solve the hierarchy problem because the Plank mass is replaced by the scale parameter M_s which is of the order of several TeV. In this model the $e^+e^- \rightarrow \gamma\gamma$ differential cross-section becomes

$$\frac{d\sigma}{d\Omega} = \left(\frac{d\sigma}{d\Omega}\right)_{\text{Born}} - \alpha s\frac{\lambda}{M_s^4}(1 + \cos^2\theta) + \frac{s^3}{8\pi}\frac{\lambda^2}{M_s^8}(1 - \cos^4\theta), \qquad (4)$$

where λ is usually assumed to be ± 1.

The t-channel excited electron exchange is introduced replacing the electron propagator (Fig.1) by an excited electron e*. This modifies the differential cross-section as follows [5]:

$$\frac{d\sigma}{d\Omega} = \left(\frac{d\sigma}{d\Omega}\right)_{\text{Born}} +$$

$$\frac{\alpha^2 \pi}{2} \frac{f_\gamma^4}{\Lambda^4} M_{\text{e}^*}^2 \left[\frac{p^4}{(p^2 - M_{\text{e}^*}^2)^2} + \frac{q^4}{(q^2 - M_{\text{e}^*}^2)^2} + \frac{s^2 \sin^2\theta}{2(p^2 - M_{\text{e}^*}^2)(q^2 - M_{\text{e}^*}^2)} \right], \quad (5)$$

where Λ is the compositeness scale, M_{e^*} is the mass of the excited electron, and $2p^2 = -s(1 - \cos\theta)$, $2q^2 = -s(1 + \cos\theta)$. The parameter f_γ is usually assumed to be 1. It should be noted that the excited electron can be directly discovered if the collider energy is sufficient to produce it. At the same time, the distortions of the differential cross-section can be observed for the excited electron masses much larger than the beam energy.

As it was shown above, the contributions of new physics modify both total and differential cross-sections of the $e^+e^- \to \gamma\gamma$ reaction. To reach the best experimental sensitivity the differential cross-section $d\sigma/d\Omega$ has to be compared with the QED predictions. The absolute normalization will be provided by CLIC luminosity which is planned to be measured with $(0.5-1)\%$ precision. Limits on the BSM model parameters will be set in a case if no deviation from QED is observed. A quick generator-level analysis shows that the LEP limits [6] on the new physics scale can be improved by more than an order of magnitude, see Table 1. This rough estimate has to be confirmed by a more detailed study. The JINR group will analyze the $e^+e^- \to \gamma\gamma$ process using the full detector simulation and reconstruction for signal and background events.

Table 1: Exclusion limits on new physics, achieved at LEP and expected for CLIC

	LEP limit	CLIC expectation
$\Lambda_\pm$ (QED cut-off)	364 GeV	6-6.5 TeV
Electron radius	4.6×10^{-17} cm	$(3 - 3.5) \times 10^{-18}$ cm
Λ' (contact interactions)	831 GeV	18-20 TeV
M_s (extra dimensions)	933 GeV	15-17 TeV
M_{e^*} (excited electron)	248 GeV	4.5-5.0 TeV

3 Precision measurement of the Higgs boson mass

Currently the Higgs boson mass (M_H) is known with a relatively low precision of about 240 MeV (combined LHC Run-1 result), to be compared with 2 MeV for Z boson (combined LEP result) or 15 MeV for W boson (PDG average of LEP and Tevatron results). It is expected that in the future LHC can reach the precision of 100 MeV or slightly better. Further improvement is necessary because theoretical predictions of exclusive Higgs decay modes are very sensitive to the Higgs mass used in the calculations. For example, for the $H \rightarrow ZZ^*$ channel the relative uncertainty of the calculated branching fraction is $\Delta BR(H \rightarrow ZZ^*)/BR(H \rightarrow ZZ^*) \approx 7.7\Delta M_H/M_H$. A 15 MeV uncertainty on M_H is required to reach a permille-level precision on partial decay width calculations.

At hadronic machines M_H is measured by direct reconstruction of the invariant mass of Higgs boson decay products. In this approach the precision is systematically limited by the calibration of particle energy scale. At e^+e^- colliders the Higgs boson mass can be determined using the process $e^+e^- \rightarrow ZH \rightarrow \mu\mu H$. M_H is reconstructed as the mass recoiling against the precisely measured $\mu\mu$ system. The decays of the Higgs boson itself are not used at all. A good knowledge of the kinematics of the initial system is necessary to use this method. At circular colliders and at ILC the experimental conditions are sufficient to measure M_H with 15-20 MeV precision. At CLIC the situation is much more challenging. Because of the photon radiation in the strong accelerating field, a large fraction of collisions occurs at energies significantly below the nominal energy. In addition, the beam energy spread at CLIC is expected to be 2 times larger than at ILC. As a consequence, the 4-momentum of the initial e^+e^- system is known with a rather large uncertainty, which translates into 110 MeV uncertainty on the Higgs boson mass [7]. A comparison of recoil mass distributions at ILC and CLIC is shown in Fig.3. The effects of the beam energy spread and of the large radiative tail are evident.

JINR group proposes to measure the Higgs boson mass using a relatively new method [8]. In this method neither the kinematics of the initial
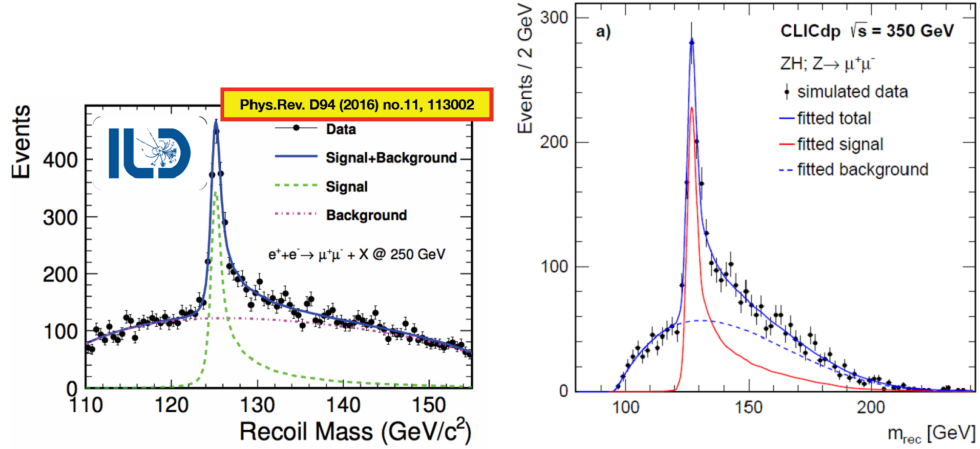
Figure 3: Recoil mass distribution in $ee \rightarrow \mu\mu H$ events for ILC (left) and CLIC (right). Note that the horizontal scales are different by a factor of 4.

collision nor the energies of the Higgs decay products are used for the M_H reconstruction. The analyzed process is $e^+e^- \rightarrow ZH$ with subsequent decays $Z \rightarrow \mu\mu$ and $H \rightarrow bb$. The muon track measurement provides a precise determination of the Z boson 4-momentum, while only **directions** (but not energies) are measured for the b-jets. To obtain a unique solution, one has to apply an additional constraint: the transverse momentum of the beam particles is assumed to be zero, which is a good approximation. The longitudinal momenta of the beam particles are not used in the reconstruction. The momenta $p_{1,2}$ of the b-jets from the Higgs boson decay can be calculated as follows:

$$p_1 = \frac{p_T^{\mu\mu}}{\sin\theta_1} \frac{\sin(\phi_2 - \phi^{\mu\mu})}{\sin(\phi_2 - \phi_1)}$$
$$p_2 = \frac{p_T^{\mu\mu}}{\sin\theta_2} \frac{\sin(\phi_1 - \phi^{\mu\mu})}{\sin(\phi_1 - \phi_2)}, \tag{6}$$

where θ_i, ϕ_i are the measured polar and azimuthal angles of the b-jets and $p_T^{\mu\mu}, \phi^{\mu\mu}$ are the transverse momentum and the azimuthal angle of the Z boson measured using the muon tracks.

7

The scheme of the method is illustrated in Fig.4. Fig.5 shows the results obtained in [8] for the ILC running. The new method has the obvious advantage over the determination of the recoil mass and direct reconstruction of the jet-jet invariant mass. This advantage is expected to be even stronger for the CLIC conditions, where the beam energy spread is larger and the beamstrahlung tail is more pronounced.
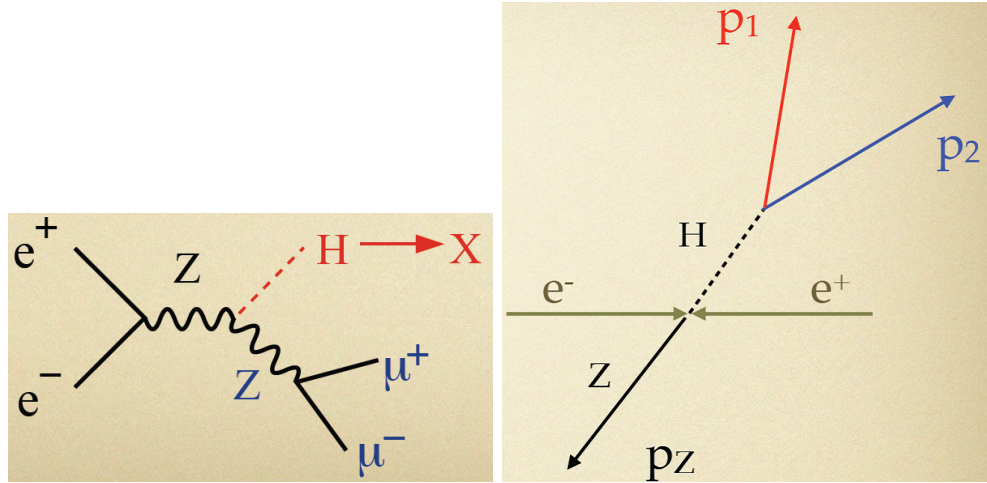

Figure 4: A scheme of the Higgs boson mass determination

The JINR group will perform a detailed study of performance of the new method in CLIC conditions. The analysis relies on precise reconstruction of hadronic jets, b-jet identification (b-tagging), and knowledge of the transverse momentum spectra of the incoming beams. Therefore, our study will be based on the full simulation of the beam delivery system and the detector response, as well as on advanced algorithms of the event reconstruction.

4 Determination of the top quark polarization

In general, the production of fermion-antifermion pairs $e^+e^- \to f\bar{f}$ is characterized by three observables: total production cross-section σ^{ff}, forward-
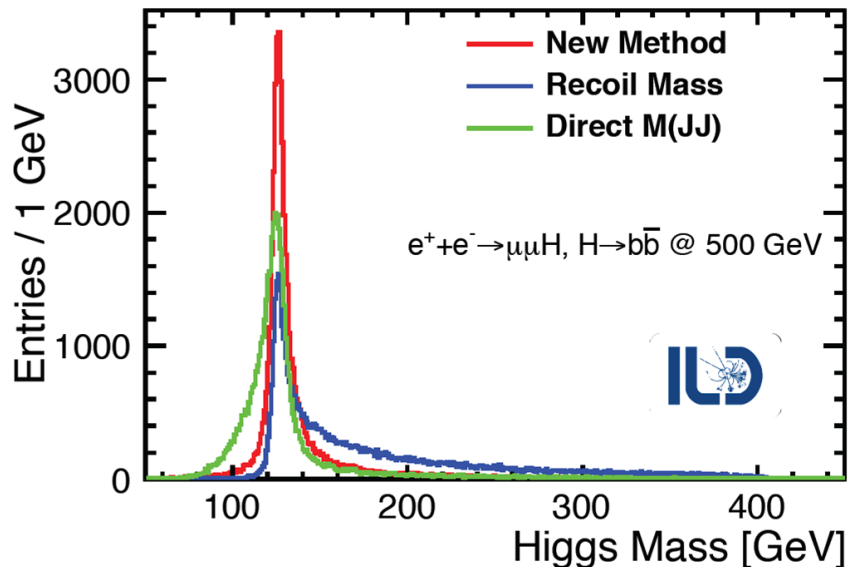
Figure 5: Distributions of Higgs boson mass reconstructed with different methods

backward charge asymmetry A_{FB}^{ff} and the average fermion polarization $P^f = (N_R - N_L)/(N_R + N_L)$, where $N_{R,L}$ are the numbers of fermions with right- and left-handed helicities. A measurement of the total cross-section is relatively straightforward as soon as a flavour identification is available (lepton identification, b- and c-tagging, etc). Charge asymmetry can be measured if the fermion charge is known. Semileptonic decays can be used to tag the charge of heavy quarks. For light quarks the momentum-weighting technique is used to estimate the "jet charge" related to the charge of the initial quark. The measurement of the fermion polarization is more complicated since usually P^f is only accessible via the kinematical correlations of the fermion decay products.

The polarization of final state electrons (stable) and muons ("almost stable") can not be measured at the multi-GeV colliders. The quark polarization is almost completely washed out in the process of hadronization. Thus, the polarization measurement is only possible for tau leptons and for the top quarks which decay before the hadronization.

The tau polarization was extensively measured at LEP. It provided a vital input to the global electroweak fit, which finally resulted in a prediction of the Higgs boson mass, $114 < M_H < 161$ GeV. In particular, one of authors of this Project has participated in tau polarization measurement at LEP-1 [9] and performed the world only P^τ measurement at LEP-2 energies [10]. In this Project the JINR group proposes a measurement of the top quark polarization at multi-TeV energies.

4.1   Top quark electroweak formfactors

The fermion production observables (σ, A_{FB}, P) can be expressed via the fermion electroweak formfactors F. For the electron beam polarisation $I = L, R$ this relation is following:

$$\sigma_I = 2AN_c\beta\left[(1 + \gamma^{-2}/2)(F_{1V}^I)^2 + (\beta F_{1A}^I)^2 + 3F_{1V}^I F_{2V}^I\right], \qquad (7)$$

where β, γ are the speed and the Lorenz-factor of the fermion, N_c is the number of colors and $A = \pi\alpha^2/3s$;

$$(A_{FB})_I = \frac{-3\beta F_{1A}^I(F_{1V}^I + F_{2V}^I)}{2[(1 + \gamma^{-2}/2)(F_{1V}^I)^2 + (\beta F_{1A}^I)^2 + 3F_{1V}^I F_{2V}^I]}; \qquad (8)$$

$$\frac{1 + (P^f)_I}{2} =$$

$$\frac{(F_{1V}^I)^2(1 + \gamma^{-2}/2) + (\beta F_{1A}^I)^2 + 2\beta F_{1V}^I F_{1A}^I + F_{2V}^I(3F_{1V}^I + 2\beta F_{1A}^I) - \beta F_{1V}^I Re(F_{2A}^I)}{2[(1 + \gamma^{-2}/2)(F_{1V}^I)^2 + (\beta F_{1A}^I)^2 + 3F_{1V}^I F_{2V}^I]} \qquad (9)$$

The electroweak formfactors F_{ij}^I can be expressed in terms of the formfactors describing ttZ and $tt\gamma$ vertices:

$$F_{ij}^L = -F_{ij}^\gamma + \frac{s_w^2 - 1/2}{s_w c_w}\frac{s}{s - m_Z^2}F_{ij}^Z, \qquad F_{ij}^R = -F_{ij}^\gamma + \frac{s_w^2}{s_w c_w}\frac{s}{s - m_Z^2}F_{ij}^Z, \quad (10)$$

where s_w and c_w are the sine and the cosine of the Weinberg angle. At Born level, Standard Model predicts the following values of the formfactors:

$$F_{1V}^{\gamma} = -2/3, \quad F_{1V}^{Z} = -(1 - 8s_w^2/3)/(4s_w c_w), \quad F_{1A}^{Z} = 1/(4s_w c_w), \quad (11)$$

and the remaining formfactors are zero within SM. If the measured cross-sections, asymmetries and polarisations deviate from the Standard Model prediction, the observed effects can be parametrized in terms of the above formfactors. In particular, two of the formfactors are related to the anomalous magnetic moment $(g - 2)$ and electric dipole moment d of the top quark: $F_{2V}^{\gamma} = q_t(g - 2)/2$ and $d = eF_{2A}^{\gamma}/(2m_t)$.

4.2 Determination of the top quark polarisation

The simplest observable sensitive to the top quark polarization is the direction of the lepton ℓ (electron or muon) from the semileptonic final state $e^+ e^- \to t\bar{t} \to (bqq')(b\ell\nu_\ell)$. The helicity angle θ_{hel} is defined as the angle in the top rest frame between the lepton direction and the vector of the top boost. The distribution of the helicity angle is defined by the top quark polarisation:

$$\frac{1}{\Gamma}\frac{d\Gamma}{d\cos\theta_{hel}} = \frac{1 + P^t\cos\theta_{hel}}{2} \quad (12)$$

At the highest CLIC energies (3 TeV) the top pairs are reconstructed as two narrow, nearly back-to-back hadronic jets. A b-tagging will be applied to both jets to reduce the background from pairs of u/d/s/c quarks. One of the jets (the one from a purely hadronic top decay) must contain a substructure consisting of three smaller sub-jets. The second jet has no substructure and is accompanied by an energetic lepton which is used to tag the top charge and to reconstruct the helicity angle. To assign the lepton to a proper jet a kinematic fit will be performed taking into account the missing transverse momentum due to the undetected neutrino.

A sensitivity study for the ILC project has been reported in [11]. The distribution of the reconstructed helicity angle is presented in Fig.6. Events follow a linear distribution function and the average top quark polarisation can be determined as the slope of the measured distribution. The expected

uncertainty $\Delta(P^t)$ is of the order of 0.01. A combination of the charge asymmetry and the polarisation measurements can improve the expected LHC limits on anomalous top formfactors by 1-2 orders of magnitude, see Fig.7. For CLIC we expect even better precision since the integrated luminosity will be larger by at least a factor of 5 and the boosted kinematics at high energies makes the top pair reconstruction easier.
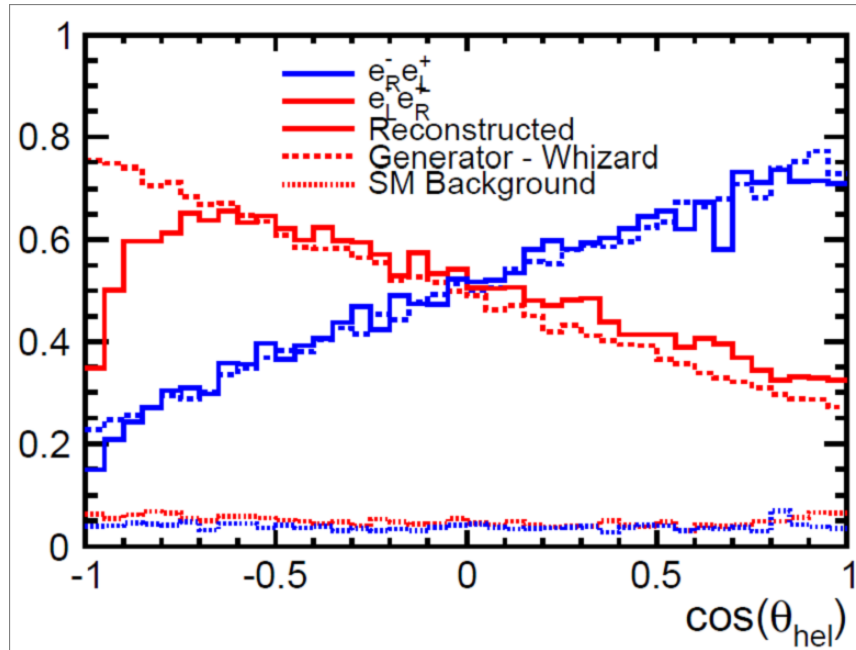

Figure 6: Distributions of the helicity angle in top quark decays for different signs of beam polarisation

5 Study of vector boson pair production in $\gamma\gamma$ collisions

Within the Standard Model the gauge boson self-interaction not only includes the tri-linear $WW\gamma$ and WWZ vertices but also quartic couplings $WWWW$, $WWZZ$, $WW\gamma\gamma$ and $WWZ\gamma$. In particular, pairs of W bosons can be produced in photon collisions $\gamma\gamma \to W^+W^-$. At the same time, the
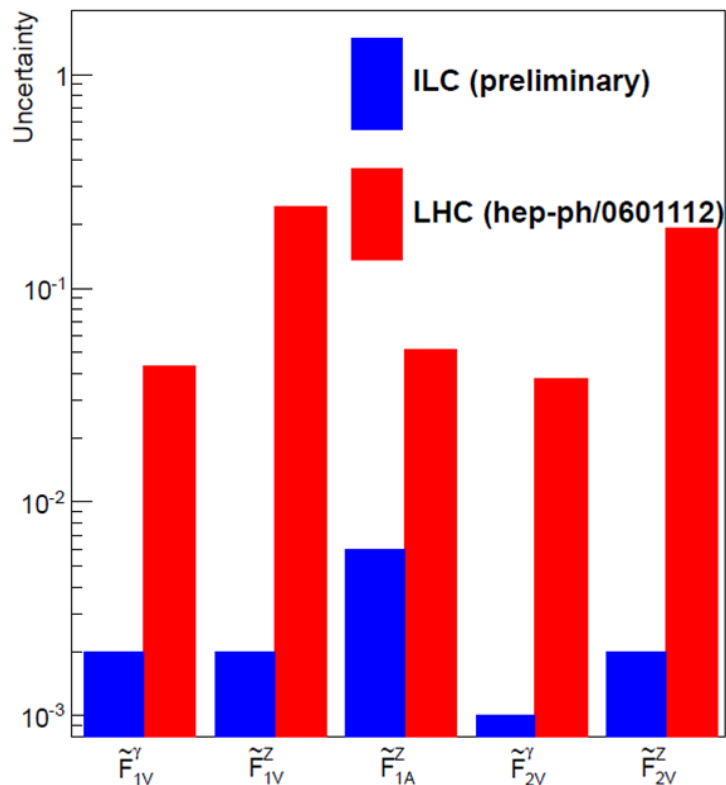
Figure 7: Comparison of LHC and ILC sensitivity to different top quark formfactors (from [11])

process $\gamma\gamma \to ZZ$ is forbidden in SM at tree level, hence an observation of this process with non-negligible cross-section would be a clear sign of BSM effects. Another way to search for new physics is to study the processes allowed in Standard Model looking for small deviations from the SM predictions. The quartic couplings are of particular interest because some theories (for example, BESS model [12]) predict new physics in quartic vertices while agree with SM in the sector of triple gauge coupling.

Quartic vector boson couplings have been studied at LEP with $e^+e^- \to W^+W^-\gamma$ channel. The obtained results allowed to exclude new physics effects at energy scales up to few GeV [13]. The poor sensitivity was due to running at collision energies close to the threshold. LHC improved the

exclusion limits on new physics scale to 100-200 GeV [14]. CLIC, with its energy much higher than at LEP and experimental environment much cleaner than at LHC, offers a possibility to improve the sensitivity by a big factor in comparison with previous experiments.

5.1   Two photon collisions at CLIC

At CLIC, due to its very strong accelerating field, a significant fraction of the beam particles will radiate a hard photon before reaching the collision point. In general this effect is considered as a disadvantage: it reduces the effective energy of e^+e^- collisions and gives rise to a pile-up background from $\gamma\gamma \to$ hadrons events. At the same time, the collisions of radiated photons can be used to study a variety of processes that occur in $\gamma\gamma$ collisions.

Fig.8 compares the CLIC luminosity spectra for e^+e^- and $\gamma\gamma$ collisions at 3 TeV nominal collision energy. As one would expect, most e^+e^- collisions occur at high energies close to the nominal one, while the spectrum of $\gamma\gamma$ collisions drops at high energies. Nevertheless, a significant fraction of $\gamma\gamma$ collisions occurs at rather high energies. The total $\gamma\gamma$ luminosity is approximately 68% of e^+e^- luminosity. If a cut $\sqrt{s} > 2M_W$ is imposed on collision energy, this ratio becomes 27%, still sufficient for a copious production of WW pairs in $\gamma\gamma$ collisions.
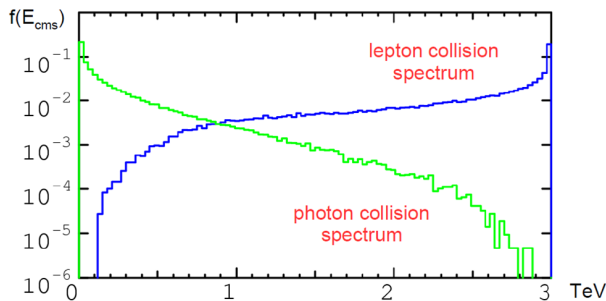

Figure 8: The fraction of *ee* (blue line) and $\gamma\gamma$ (green line) collisions versus the collision energy for the 3 TeV CLIC running.

14

Fig.9 compares the cross-sections of W pair production in electron-positron and in $\gamma\gamma$ collisions. Even taking into account the 27% luminosity ratio one concludes that for the high-energy CLIC running the majority of W pairs will be produced in $\gamma\gamma$ rather than in e^+e^- collisions. The abundance of $\gamma\gamma \to W^+W^-$ events provides a very good sensitivity to the quartic $WW\gamma\gamma$ coupling.
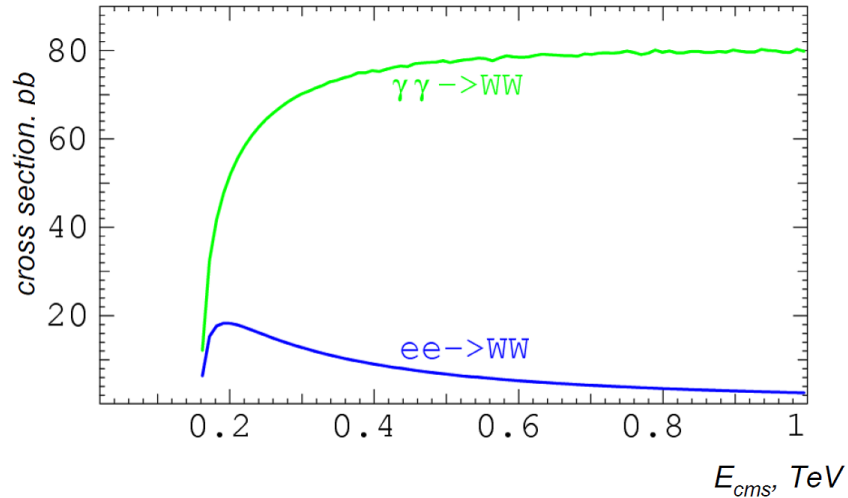

Figure 9: Cross-section of W pair production in electron-positron and in $\gamma\gamma$ collisions versus the collision energy.

5.2 Study of $\gamma\gamma \to W^+W^-$ events

The simplest way to select $\gamma\gamma \to W^+W^-$ events is to use the purely leptonic $e\mu$ final state. This channel has relatively small branching fraction, which is compensated by the very high purity of the signal, since only few Standard Model processes result in the same final state.

The statistics can be increased by including tau leptons, same-flavour lepton pairs and semi-leptonic final states $WW \to qq'\ell\nu_\ell$. These channels require a detailed full-simulation study which will be performed in the framework of this Project. Here we only discuss a quick generator-level analysis which shows that even the $e\mu$ channel alone is very promising.

15

Fig.10 shows the energy dependence of the cross-section for the signal process $ee \rightarrow WW \rightarrow e\mu$ and for the background processes with the same $e\mu$ final state and with e^+e^- final state. A cut $\theta > 10°$ on polar angle acceptance was applied to take care of Bhabha cross-section divergence. The cross-section for signal is significantly higher than for all $e\mu$ backgrounds. The Bhabha cross-section is 2 orders of magnitude higher than the signal, however the e/μ separation is expected to have the purity much better than 99%.
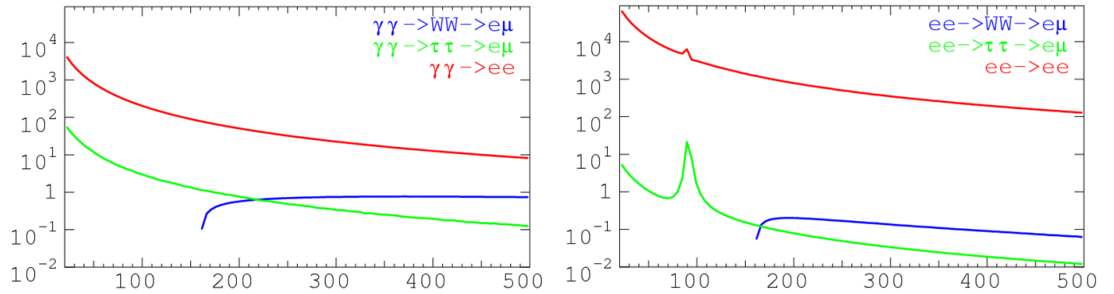

Figure 10: Energy dependence of signal and background cross-section for $\gamma\gamma$ (left) and ee (right) collisions. Energy is in GeV and cross-sections in picobarns.

Fig.11 shows the distribution of the invariant mass of the $e\mu$ system. The signal is compared with all sources of $e\mu$ background. Event numbers are normalized to 1000 fb^{-1} integrated luminosity for the 3 TeV CLIC running. The total background is at the level of 10% of the signal. At high masses the signal drops due to the cut-off of the $\gamma\gamma$ spectrum. However, even at highest invariant masses the signal-to-background ratio is expected at the level of 1:1.

5.3   Limits on the anomalous quartic coupling

The $WW\gamma\gamma$ anomalous quartic coupling can be parametrized by adding an anomalous term to the Standard Model Lagrangian $\mathcal{L}_{SM}$ [15]:
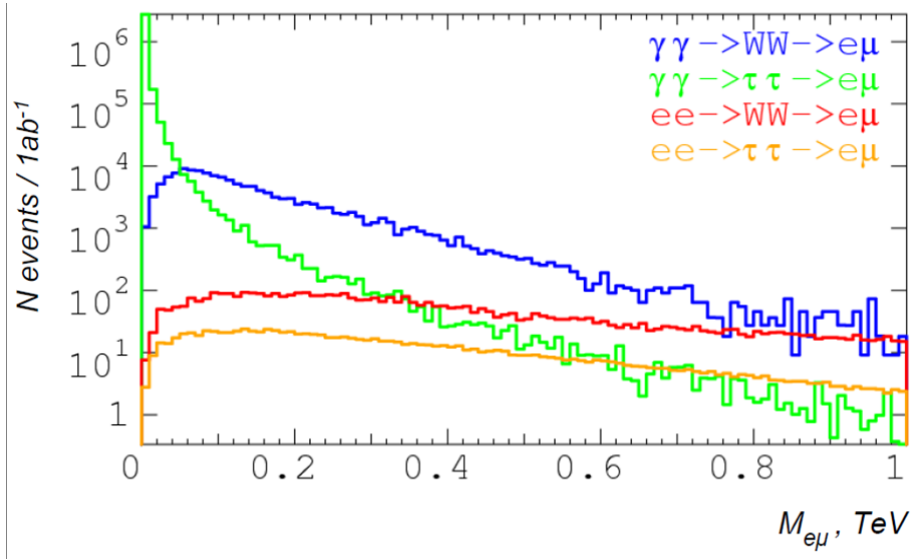
Figure 11: Distribution of invariant mass of the $e\mu$ system for signal and background events.

$$\mathcal{L} = \mathcal{L}_{SM} - \frac{e^2}{16\pi\Lambda^2}a_0 F_{\mu\nu}F^{\mu\nu}W^{\alpha}W_{\alpha} - \frac{e^2}{16\pi\Lambda^2}a_c F_{\mu\alpha}F^{\mu\beta}W^{\alpha}W_{\alpha}, \qquad (13)$$

where Λ is the typical energy scale of the new physics effects.

The generator-level estimate of signal and background yield in the $e\mu$ channel was used to estimate limits on a/Λ^2 parameters. In Fig.12 the results are compared with the results from CMS [14]. The expected improvement is by more than 2 orders of magnitude (equivalent to more than one order of magnitude in energy scale). Note that our results are based on a generator-level study and represent only a very rough estimate. A detailed full-simulation analysis will be performed in the framework of this Project.

The sensitivity to the anomalous coupling $ZZ\gamma\gamma$ might be expected to be even better than to $WW\gamma\gamma$, because there is no Standard Model background $\gamma\gamma \rightarrow ZZ$ at the tree-level. It is difficult to estimate the sensitivity for such "zero signal" channel with a quick generator-level study.
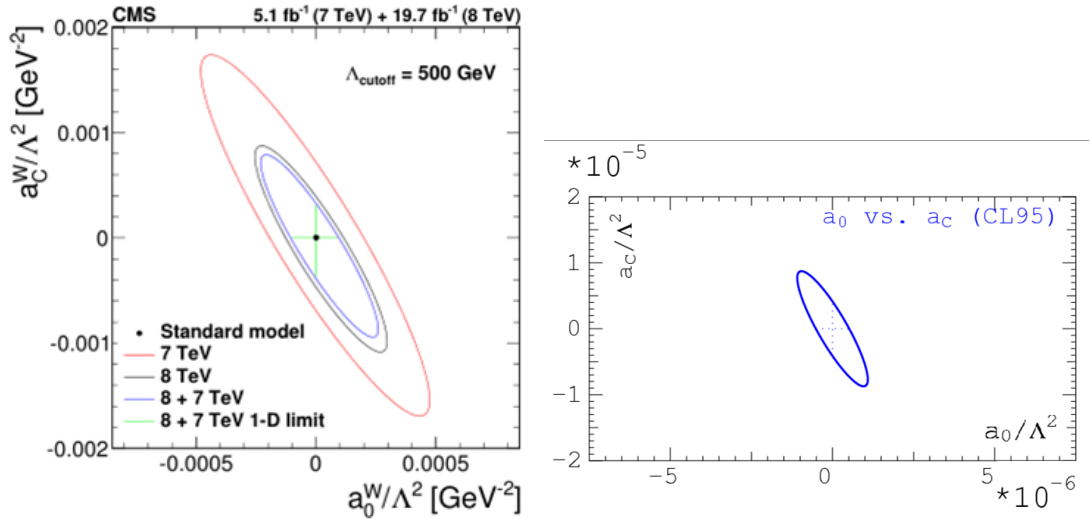
Figure 12: CMS exclusion limits on anomalous coupling constants (left) and exclusion limits expected for CLIC (right).

A full-simulation study of the $\gamma\gamma \to ZZ$ channel is planned to be performed in the framework of this Project.

6 Summary on participation in the CLIC experimental program

CLIC is planned to be operated at several energies ranging from 350 GeV to 3 TeV. Already at the first energy stage the expected CLIC results are similar to other e^+e^- collider projects. Operated at its highest energy, CLIC is unbeatable in sensitivity to the tiny effects of the new physics phenomena.

In this project we propose to complete a detailed study of CLIC potential in four different fields. For two of them, $e^+e^- \to \gamma\gamma$ and $\gamma\gamma \to W^+W^-$ processes, CLIC is expected to perform much better than any other proposed e^+e^- collider. For the measurement of top quark polarisation CLIC sensitivity is expected to be similar or slightly better than at ILC. As to

the measurement of the Higgs boson mass, the CLIC precision is currently estimated to be at least 5 times worse than for other e^+e^- collider projects. We propose to investigate a new method of M_H measurement which is expected to improve the precision very significantly. Even if the expected precision can not reach the level of CLIC competitors, still the new result would be an important input for the choice between different projects.

References

[1] W. Heitler, Quantum Theory of Radiation, Oxford University Press (1944) p.204-207

[2] S.Drell, Annals Phys. 4 (1958) 75-80
F.Low, Phys. Rev. Lett. 14 (1965) 238-239

[3] O.J.P.Eboli, A.A.Natale, and S.F.Novaes, Phys. Lett. B271 (1991) 274

[4] I.Antoniadis et al., Phys.Lett. B436 (1998) 257-263

[5] B. Vachon, hep-ph/0103132, 2001

[6] The LEP Collaborations, "A Combination of Preliminary Electroweak Measurements", arXiv:hep-ex/0612034

[7] CLIC coll., H.Abramovicz et al., Eur.Phys.J. C77 (2017) 475

[8] Tian JunPing, "Measurement of the Higgs boson mass", a talk given at the LCWS17 workshop, Strasbourg, October 2017

[9] I.R.Boyko, "A measurement of cross-sections, asymmetries and polarisations of tau leptons", Ph.D. thesises, Dubna, 2002 (in Russian).

[10] DELPHI coll., J.Abdallah, et al., Phys.Lett. B659 65-73, 2008

[11] M.S.Amjad et al, "A precise determination of top quark electro-weak couplings at ILC", arXiv:1307.8102

[12] R. Casalbuoni, S. de Curtis, D. Dominici and R. Gatto, Nucl.Phys. B282 (1987) 235

[13] L3 coll., P.Achard et al., Phys.Lett. B527 (2002) 29-38

[14] CMS coll., V.Khachatryan et al., JHEP 1608 (2016) 119

[15] M.Baak et al., "Study of Electroweak Interaction at the Energy Frontier", arXiv:1310.6708